Bifurcations to chaos in optical bistability

F. A. Hopf, D. L. Kaplan, H. M. Gibbs, and R. L. Shoemaker
University of Arizona, Optical Sciences Center, Tucson, Arizona 85721
(Received 28 September 1981)

The details of the time-dependent output from a hybrid optical bistable device are investigated in the regime where the delay time of the feedback signal is much larger than the response time of the device (determined by electrical bandwidth of the feedback loop). The delayed feedback is produced by placing a computer equipped with fast *A-D* and *D-A* converters in the feedback loop. This bistable system exhibits periodic and chaotic instabilities as predicted by Ikeda. In particular, as the input intensity is increased, the device output goes through a series of bifurcations (second-order nonequilibrium phase transitions). First, the initially stable output changes to a periodic output (a square wave) followed by a second periodic region whose period is twice that of the previous region. Up to this point, the system behavior is in agreement with the period-doubling scheme of Feigenbaum. However, the period doubling which is predicted next is only rarely observed. Instead the system usually goes over into chaotic behavior. Within the chaotic region, the device largely follows the reverse bifurcation scheme of Lorenz. In addition, there is a small domain of frequency-locked behavior that exists within the chaotic domain. These bifurcations are not only of fundamental interest but may find applications in practical optical devices.

I. INTRODUCTION

The nature of chaos, or equivalently of turbulence, has been the subject of intense interest throughout the last 20 to 30 years, and has played a significant role in many diverse disciplines[1] ranging from cosmology and hydrodynamics in physics to population genetics and evolutionary biology. Recently, Ikeda *et al.*[2,3] have shown theoretically that instabilities and chaotic behavior can occur in an optically bistable[4] device due to the finite round-trip time (delayed feedback) of an optical cavity. In an earlier experiment, we used a hybrid bistable device to demonstrate that these instabilities occur, showing qualitatively that periodic and chaotic temporal behavior is exhibited in the region of instability.[5] In this paper, we examine experimentally the quantitative details of the unstable region of an improved hybrid bistable device.

The observation of chaos in optically bistable systems is interesting because of the fundamental nature of the process. It is also especially interesting relative to the general field of turbulence because the optical devices are very simple by comparison to other cases in which chaos exists.[1,6–10] As such, comparison of theory with experiment should be more straightforward than in other cases. Chaos is differentiated from noise insofar as it is a result of deterministic rather than stochastic dynamics. Chaos was originally regarded as just very complicated behavior,[11] in which case the division between chaotic and nonchaotic behavior is arbitrary. A more recent viewpoint[12] is that chaos is a distinct phase of a nonequilibrium system, and is characterized by an output that is intrinsically unstable, insofar as all allowed trajectories $X(t)$ of the system when perturbed to $X(t) + \delta X(t)$, result in an exponential growth of δX. Such detailed time trajectories are noncomputable due to the fact that the effect of round-off errors increases exponentially in time as the system evolves, although average properties such as spectra can be computed. Ikeda *et al.*[3] have shown that this feature of chaos should manifest itself in special details of the output of our device, and we find that these predictions are both correct and of great value in visually distinguishing chaotic and noisy behavior. This is discussed in detail in Sec. III.

Much of the current interest in chaos is concerned with the set of nonequilibrium phase transitions (bifurcations) which lie between the stable and chaotic behavior. We will restrict our discussion to the phases that are expected in our case, which involve limit cycles. These cycles differ from each other in that the period of the cycle is

doubled as one goes from one phase to the next in the direction of chaos.[13] Feigenbaum has recently shown that while there may be an infinite number of periodic phases in the period-doubling sequence, the domains of these phases shrink geometrically with a rate δ so that the overall domain of periodicity is finite.[14] Furthermore, he demonstrated that the rate δ is a universal property of period doubling that is largely independent of the details of the system. Previous tests of Feigenbaum's ideas have been made in hydrodynamics with mixed results. Some cases work as he predicts[8] and some do not.[7] Our system is one dimensional, as is the case that Feigenbaum analyzed, and as such, its behavior might be expected to follow his scheme closely.

In Sec. II we describe the experimental apparatus used and present the results obtained with it. In Sec. III, a discussion is given of the behavior expected theoretically using a model of the system given by a simple difference equation. The model predictions are compared to the results and over most ($\sim 98\%$) of the parameter range of our study, the agreement of experiment and theory is satisfactory. Within the 2% range of disagreement, we observe the second period doubling (called "period eight") only rarely, we never see higher period doublings, and we observe a frequency-locked output that is not predicted by the difference equation. There are two theoretical studies currently in progress[15,16] of the difference-differential equation that describes our device. These studies are not in agreement in that they lead to contradictory interpretations of our difficulties in observing period eight. One of them does find the frequency-locked behavior[15] (the other did not cover the regime in which it exists). Preliminary results from these studies are compared with the experiment in Sec. III, and further discussion of the problem is given in Appendix A. Finally, in Sec. IV, we summarize our results and discuss possible experiments which might resolve the remaining questions.

II. EXPERIMENT

The present experimental setup uses the hybrid optical bistable device shown in Fig. 1. It is largely the same as the one in Ref. 5 except that we have replaced the Pb-based lanthanum-doped zirconate titanate (PLZT) electro-optic device with a conventional potassium dihydrogen phosphate (KDP) modulator and have used a different value of dc bias. PLZT has an intrinsic hysteresis which

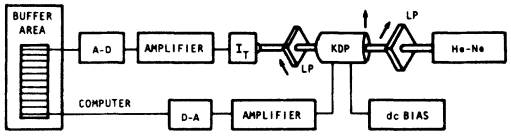

FIG. 1. Experimental layout: He-Ne; LP, linear polarizers (crossed); KDP, modulator; I_T diode that measures transmitted light (the experimental output is taken at this point). The other items are self-explanatory.

influences the details of the system response in a complicated fashion. With the new modulator, we find that the bifurcation structure is much simpler and is also in much better agreement with theory. The key element that produces the instability is a time delay in the feedback loop which plays the role of the cavity round-trip time t_R in an intrinsic bistable device. We produce the delay by feeding the output of the detector through an A to D converter into a TRS80 computer. The signal is sampled every 0.225 msec. The result is stored in a buffer in memory and is then fed back through a D to A converter to the modulator at a time t_R later. The two amplifiers in Fig. 1 are needed to match the voltage requirements of the computer to those of the detector and the modulator.

The equation that describes this bistable device is[3]

$$\tau\dot{X}(t)+X(t)=\pi\mu\{\,1-\xi\cos[X(t-t_R)+X_b]\}\,, \tag{1}$$

where $X=\pi V/V_h$, V is the voltage fed to the modulator, V_h is the half-wave voltage of the modulator $X_b=\pi V_b/V_h$ is the bias, τ is the response time of the electronic circuit, and ξ is a coefficient that measures the ability of the modulator to achieve extinction between the crossed polarizers. The bias is set so that $X_b=-\pi/2$ to within 1% (note that in the previous experiment, the bias was set close to zero). The coefficient ξ is nearly unity (we measured $\xi=0.98\pm0.01$). The bifurcation parameter $\mu=CG_1G_2I_{\rm in}$ is proportional to the gains G_1 and G_2 of the amplifiers and to the input laser intensity $I_{\rm in}$, and is the parameter that is varied in the experiment. The constant μ is measured directly by breaking the feedback loop between the final amplifier and the modulator. A zero voltage is placed on the modulator and a voltage V is measured at the output of the final amplifier. From Eq. (1) this gives $\mu=V/V_h$.

Ikeda showed theoretically[3] and we confirmed experimentally[5] that instabilities associated with

the difference term in Eq. (1) occur whenever $\tau << t_R$ (i.e., the "good cavity" limit of optical bistability), while $\tau >> t_R$ leads to conventional stability criteria for the device. We normally use $t_R = 36$ msec and $\tau = 0.8$ msec so that $\tau << t_R$. In that case, it seems reasonable to suppose that much can be learned about the behavior of the device by dropping the term $\tau \dot{X}$ from Eq. (1), defining $t_n = nt_R$, $X_n = X(t_n)$, and using the nominal fixed values of $\xi = 1$ and $X_b = -\pi/2$ to obtain

$$X_{n+1} = \pi\mu(1 - \sin X_n) . \tag{2}$$

A primary concern is the question of how well Eq. (2) predicts the output of the experiment. This is discussed in Sec. III.

The remainder of this section is divided into two parts. In the first subsection we describe the major results of the experiment insofar as they deal with the issues of period doubling and chaos. In the second subsection we discuss the features of the experiment that relate to optical bistability.

A. Bifurcations and chaos

The basic experimental quantity of interest is the time-dependent output of the bistable device shown in Fig. 2. We also take the power spectrum of the output voltage and make histograms of the function $X(t)$.

Since the computer is mostly inactive during the 100 μsec required for an A to D conversion, we can use it to make the histograms of the output voltage. The voltage is digitized to eight-bit accuracy and each voltage is associated with a sixteen-bit location in memory. We add one to the appropriate location in memory at each digitization step. The histogram is regarded as complete whenever any voltage is recorded 2^{16} times. Since we digitally sample the waveform at a rate which is four times the highest frequency present, there are approximately 2^{14} statistically independent samples. The data are then combined to conform to the 48 $\times$ 128 graphics display of the cathode-ray tube (CRT). This corresponds to about 10^3 points for

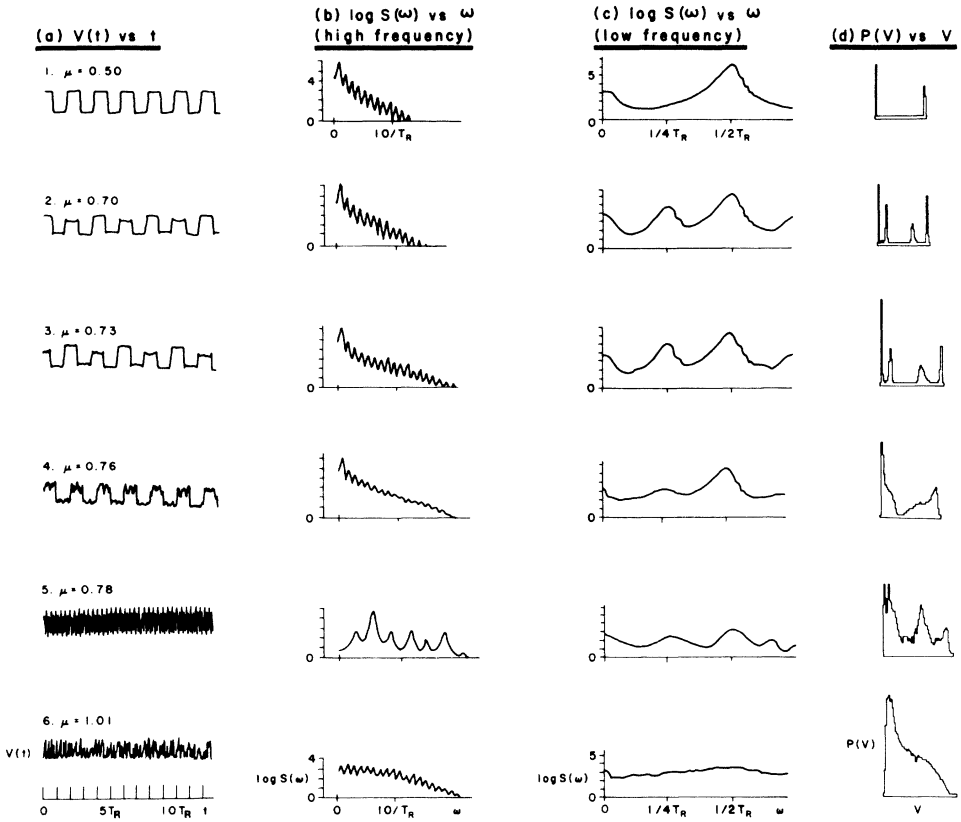

FIG. 2. Basic time-dependent outputs of the device taken from the lower branch. The rows are the data for different input intensities labeled by the measured value of μ. The columns are (a) A sample of voltage V arbitrary units vs time in units of t_R. (b) The log of the spectrum of V vs ω on a coarse scale. (c) The log of the spectrum on a fine-frequency scale. (d) The histogram of the output voltage on an arbitrary scale.

each unit on the vertical scale which means that the maximum statistical error in the histogram is about 3%. We record the time trace on a tape-recorder so that we can subsequently take the power spectrum of the time trace that gave the histogram. The value of μ is also measured with an accuracy of $1-2\%$. We normally measure μ first, allow all transients to die away, and then take the histogram and the time trace. We then measure μ again to insure against drift of the laser power.

Since our spectrum analyzer is unable to handle the relatively slow time scales of the device, we speed up the trace with variable speed tape-recorders. The sped-up trace is fed into the spectrum analyzer and the output of the spectrum analyzer is digitally averaged for greater accuracy. During the recording of the trace, the dc component is altered so that in all spectra its value is arbitrary and is greatly reduced below its real value.

In Fig. 2 we give representative examples of the time dependence and statistics for the six major time-dependent features of the device output and the values of μ at which they were measured. Note that all of these features come from the *lower* branch of the conventional optical bistability hysteresis curve (transmitted intensity vs. input intensity) as is discussed further in Sec. III. These features are observable even when a few of the optical components are misaligned, or when the range of voltages fed to the A to D converter is too small which significantly increases the noise level. The four columns in Fig. 2 are

(a) voltage in arbitrary units versus time in units of t_R,

(b) power spectrum on a logarithmic scale versus frequency on a scale from zero to $20/t_R$,

(c) power spectrum, again on a logarithmic scale versus frequency with the abscissa expanded to show the low-frequency behavior,

(d) histogram with arbitrary scales showing the probability of a given X vs X.

Row one shows the square wave whose period is, as expected, close to the value $\sim 2(\tau+t_R)$, where the factor of two in the period is responsible for the nomenclature "period two." Row two shows the output of the first period doubling which is called "period four." Note that while the period two is a nice square wave, there are overshoots of the middle amplitudes of the period four. These may be of significance in the nonobservance of periods eight.[16] Note in the spectra that the subharmonics associated with period four are much smaller than the period-two peaks; this is in agreement with theory,[14] both qualitatively and quantitatively (see Appendix A). The width of all spectral peaks in rows one and two are instrumentally limited and the background noise is very low. The spectrum in row one (broad scale) is in good agreement with the periodic example in Ref. 3.

Rows three, four, and six correspond to outputs that we call "period-four chaos", "period-two chaos," and "period-one" or "fully developed chaos," respectively. Note in the time trace the rapid time scale on which the chaos occurs. This is due to the unstable character of chaotic trajectories,[3] and is why chaotic traces can be readily distinguished from noisy traces. Note also that, in agreement with theory,[17] the period-four chaos appears to be similar to the period-four case with a small chaotic background. The histogram of period-four chaos has four distinct domains of nonzero amplitude and three well-defined domains of essentially zero amplitude. In the passage from period-four to period-two chaos, the outer two zero-amplitude domains shrink smoothly to zero width and the two lower and higher domains merge into each other. This is in agreement with theory.[17] In the passage from period-two chaos to fully developed chaos, we see that $X(t)$ can wander over the domain from $X=0$ to $X=\pi\mu$ with no gaps in the histogram. The spectra of the chaotic traces are broader overall than in the periodic cases, and while there are still peaks corresponding to period-two behavior, they have become broader (they are no longer instrument limited). The spectral background is very high and the peaks are only a factor of 10 above the background. The spectrum of fully developed chaos is in good accord with the chaotic example in Ref. 3.

The waveform shown in row five is an example of the strange waveforms that we see in a very small domain of μ between period-two chaos and fully developed chaos. The spectral peaks are governed by τ rather than t_R (changing t_R does not radically alter the main features of the spectra), and the spectrum shows only weak structure associated with t_R. Within this zone, two or three different basic waveforms are observed, each having a dominant frequency component that is locked to an odd harmonic of the period-two waveform (hence the name "frequency locked"). Only the odd harmonics whose frequencies fall within a domain approximately described by $k/\tau \pm 1/t_R$ give

rise to a frequency-locked waveform, where $k \approx \frac{1}{8}$ is an empirically determined constant. In general, these waveforms are not periodic, but occasionally, as in the example shown in row five, a high degree of periodicity may be exhibited. The waveform shown in row five has a fundamental frequency of $11/2t_R$, but it also has a substructure similar to a period-four waveform. This gives the peak at $11/4t_R$.

The domain in μ of the frequency-locked behavior is so small that we cannot reliably measure it, but it is approximately 0.01 (i.e., $< 1\%$ of the range of μ) and the subdomains of different locking frequencies are even smaller. The transients in this region are very long lived (from 30 sec to 10 min) compared to those of the periodic regime. Our laser is usually stable enough to stay within these small domains for such long times although it intermittently drifts. By comparison to these domains, the predicted size of the period-eight domain given in Sec. III is 0.016. This is certainly much larger than the frequency-locked subdomains, which is why we reject the idea that our nonobservation of period eight is due to spurious device instabilities.

B. Relationship to bistability

In this subsection, we would like to address those features of our experiment that relate to issues of optical bistability. The most important point we discuss is related to the nature of the bistable hysteresis loop measured when the output is averaged over time greater than t_R so that the instability is not directly observable. For the set of parameters chosen for this experiment, the time-average bistable loop is very different from the loop predicted when the instability is ignored. The opposite is true in the case discussed in Ref. 5. This has interesting implications for future experiments in intrinsic devices. We also note the observation of a "precipitation" phenomenon.

For values of $\mu > 1$, the upper and lower branches of our device lose their identity, both theoretically and experimentally, and the output wanders erratically between the two states. In this regime, one neither expects nor finds that the time-average power will be near either of the branches, but rather is somewhere in between. In Fig. 3, we show (a) the output voltage and (b) the time-average output voltage versus input laser intensity (horizontal axis $\equiv \mu$) as the intensity is slowly cycled from zero to a maximum ($\mu > 1$) and back to zero. To obtain Fig. 3(b), the output voltage was measured after passing through a simple low-pass resistance-capacitance (RC) filter with a large time constant so that the time transients are averaged out. The device parameters are the same as Sec. II A.

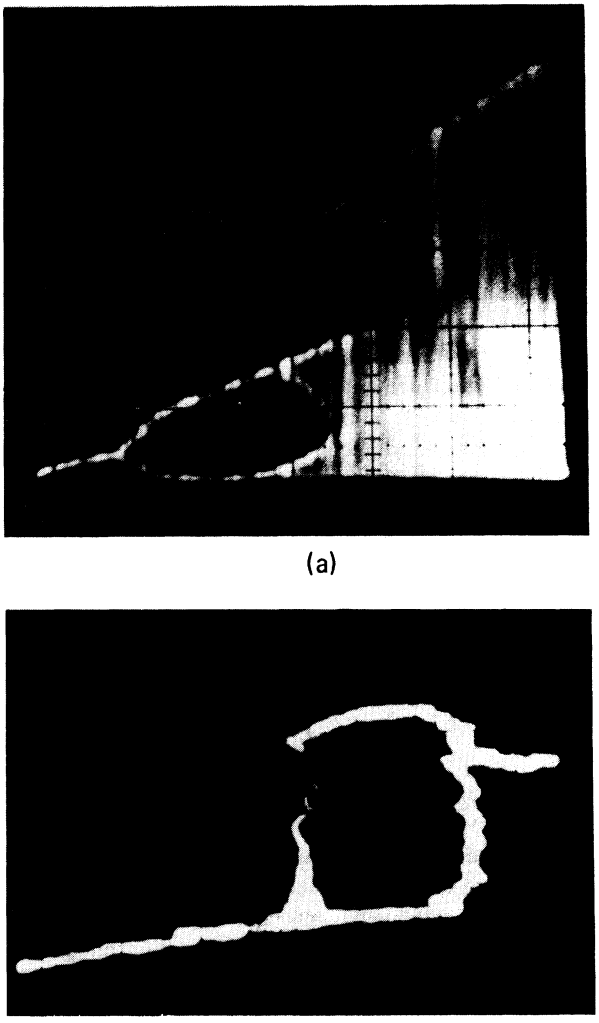

FIG. 3. (a) Output voltage V, which is mostly time dependent and hence multivalued vs input laser intensity, where the input intensity is cycled from zero to a maximum ($\mu > 0$) and back to zero. (b) Same as (a) except the vertical axis is the time average voltage on the same scale as (a).

Let us take Fig. 3(a) first. For small μ, the stable output gives a trace which is a single line. For higher μ, one gets the periodic regime in

which the output jumps between two values. This appears in the figure as a branching of the lower state. The lines then split again to give period four and beyond that there is chaos. The details of the chaotic portion are not observable here, since we cycle too quickly for the transients to settle down. The chaos involves a wandering over a domain $0 \leq X \leq \pi\mu$ and appears as a wash. Then, as intensity is increased past $\mu = 1$, the chaotic trace suddenly jumps so that it covers the domain $0 \leq X \leq 2\pi\mu$. As μ is decreased, it is a stochastic question which branch is selected. We show the case of the upper branch, in which case chaos, followed by periodic, then stable portions of the branch are observed. At $\mu \approx 0.7$, the trace returns to the lower branch where period-four motion is resumed.

The time-average power, shown in Fig. 3(b), is extremely different from what would be expected theoretically if the Ikeda instability were not present. The right-hand point where the loop closes occurs at a value of the input laser intensity which is much smaller than predicted by conventional bistability theory (see Sec. III). Moreover, the average power is manifestly not that of the upper branch, which is what conventional bistability analysis predicts. It may be possible to use this difference in the time-average output to observe an instability in an intrinsic ring device which was the original problem considered by Ikeda. The known nonlinear media with very short τ have relatively small nonlinear coefficients, and thus Q-switched lasers are needed to make nonlinearities occur. One will need short cavities to make the device have an adiabatic response to the Q-switched laser pulse, and this will make it very difficult to resolve the time dependence of the instability.

We also note that we observe an Ikeda instability even if $\tau \approx 3t_R$, although the domains of instability are greatly altered for $\tau \geq t_R$. This is encouraging from the standpoint of verifying the existence of the instability in a cavity using cw lasers. Certain materials such as Na and GaAs have response times $\tau \approx 20$ nsec and large enough nonlinearities to be used in a 2–3-m cavity with a cw laser. There should be no difficulty in resolving the time dependence of the output in this case.

When the bias is set at slightly less than $-\pi/2$, the chaotic upper state spontaneously drops into the chaotic lower state. This has been called a "precipitation."[18] This is the first experimental observation of such a phenomenon in optical bistability. Precipitation has been predicted to occur in self-pulsing instabilities[18] as well as in our case.[15] Since we have been predominantly concerned with instability in the lower branch, we often fail to ensure that the electrical system is linear in the upper state. This nonlinearity causes the upper branch to be stable for all μ considered here. In that case, for $\mu > 1$, the unstable lower state precipitates to the upper branch. This is the type of precipitation that has been predicted for self-pulsing instabilities, but in that case, it is always the lower state that is stable and the upper state which is unstable. Another interesting phenomenon occurs when the detector is slightly saturated (by using large input intensities and lower amplifier gains) while on the lower branch. We then see period-three solutions in the chaotic domain. In this case, one can find examples where both period-three and chaotic output occur for the same device setting, which is the essence of the theorem of Ref. 19, namely, that "period three implies chaos."

III. THEORY AND COMPARISON WITH EXPERIMENT

Many of the basic ideas which underly the current understanding of chaotic behavior have been generated by studying equations that are similar to Eq. (2).[1,13,14] We were motivated to choose the case $\xi = 1$ and $X_b = -\pi/2$ so as to reproduce all of the important features of the parabolic map $X_{n+1} = \mu X_n(1 - X_n)$, since it is the case that has received the greatest attention in the literature.[1]

The steady states of Eq. (2) are the same as those of Eq. (1) and are defined by $X_{n+1} = X_n = \bar{X}^{(1)}$. In Fig. 4, we show the steady state as a function of μ for $0 \leq \mu \leq 1$, which is part of the usual "S" curve of optical bistability. The lower branch continues out to a value $\mu >> 1$ where conventional theory predicts that the device should go to the upper branch [(note that this is in direct conflict with the experimentally observed loop in Fig. 3(b)]. In the experiment, we concentrated on the instabilities in the lower branch of the curve. For that reason, we do not introduce notation that differentiates the upper and lower branches. Should ambiguities arise from this notation, they are resolved by applying the results only to the lower branch. For convenience, let us denote the right-hand side of Eq. (2) as $f(X)$, and its derivative with respect to X as $f'(X)$. The steady state is then stable if and only if $|f'(X)| < 1$. The steady-state curve in Fig. 4 is divided into seg-

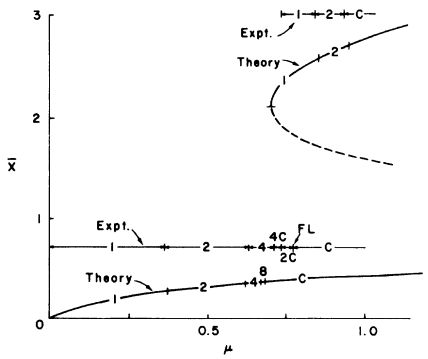

FIG. 4. The portion of the "S" curve of our bistable device over the domain $0 \leq \mu \leq 1$ of the experiment. $\bar{X}_1$ is the customary steady-state output (here mostly unstable) vs input laser intensity scaled as μ. The dashed portion is unconditionally unstable. The theoretical curve is labeled 1,2,4,8 to indicate period-one (stable), period-two, etc. Note that periods sixteen and higher on the lower branch and four and higher on the upper branch cover very small domains that are not shown. The label "C" indicates chaos. The experimental bifurcation structure is indicated along the horizontal lines. The domain of the frequency locked (FL) anomally is too narrow to be shown ($\Delta\mu < 0.01$). Note that the uncertainty of locating the bifurcation points experimentally is quite large ($\sim 5\%$) due to critical fluctuations.

ments, and only the segments labeled "1" are stable. All other portions are unstable. The dashed portion is the unstable branch which plays no role in the dynamics and is ignored from now on. If the steady-state output becomes unstable at some μ (denote this as $\mu=\mu_1$), the next equation to check is the first iterate of Eq. (2), namely, $X_{n+2}=f^{(2)}(X_n)$, where $f^{(2)}(X) = f(f(X))$. If one inspects this equation for its steady states, one finds that a bifurcation takes place at the point $\mu=\mu_1$. One finds three steady states for $\mu > \mu_1$, which we denote as $\bar{X}_i^{(2)}$, $i=1,2,3$, such that $\bar{X}_3^{(2)} = \bar{X}^{(1)}$ (i.e., the old steady state) is unstable by the stability criterion $|f^{(2)\prime}(\bar{X}_3^{(2)})| > 1$, and $\bar{X}_1^{(2)}$ and $\bar{X}_2^{(2)} = f(\bar{X}_1^{(2)})$ are stable. Because $\bar{X}_1^{(2)}$ is the iterate of $\bar{X}_2^{(2)}$, this describes a time-dependent output of the device of period two. This is labeled as "2" in Fig. 4. As one increases μ, the steady states of $f^{(2)}$ become unstable at $\mu=\mu_2$. Except for bookkeeping and notation, the analysis of the bifurcation of the period-two system is exactly the same as period one, since the initial function was arbitrary and could have been chosen to be $f^{(2)}$ in the first place. Hence, the next step involves looking at the first iterate of $f^{(2)}$, namely, $f^{(4)}(X) = f^{(2)}(f^{(2)}(X))$. This is found to bifurcate at the point $\mu=\mu_2$. One finds seven steady-state solutions of $X_{n+4}=f^{(4)}(X_n)$ of which $\bar{X}_5^{(4)} = \bar{X}_1^{(2)}$, $\bar{X}_6^{(4)} = \bar{X}_2^{(2)}$, and $\bar{X}_7^{(4)} = \bar{X}^{(1)}$ are unstable, and the timing sequence of the four stable solutions is defined by $\bar{X}_{i+1}^{(4)} = f(\bar{X}_i^{(4)})$, $i=1,2,3$ and $\bar{X}_1^{(4)} = f(\bar{X}_4^{(4)})$. At this point, it is convenient to let $\bar{X}_1^{(2)^n}$ be the smallest stable solution, in which case one finds that

$$\bar{X}_1^{(4)} < \bar{X}_3^{(4)} < \bar{X}_4^{(4)} < \bar{X}_2^{(4)} . \tag{3}$$

This establishes the basic pattern of the period-four system which we always observe experimentally. Notice also that the bifurcation is such that as $\mu \to \mu_2$, $\bar{X}_1^{(4)} \to \bar{X}_1^{(2)}$ and $\bar{X}_3^{(4)} \to \bar{X}_1^{(2)}$ (the others approach $\bar{X}_2^{(2)}$). This means that near the bifurcation point, the period-four solutions are very similar to the (unstable) period-two solutions. Note also that $0 < \bar{X}_1^{(4)} < \bar{X}_1^{(2)}$ with similar restrictions on the other stable amplitudes.

This stability analysis is then iterated through periods 8, 16 , . . . , 2^{n+1} where the bifurcation points are at $\mu=\mu_n$. One of the important theoretical advances[14] in understanding these bifurcations is the realization that the theoretical analysis of the period-2^{n+1} case can be scaled into the analysis of the 2^n case with a scaling relation that depends only on f being parabolic in the neighborhood of its critical point. Among other things, this scaling implies that

$$\lim_{n\to\infty} \frac{\mu_n - \mu_{n-1}}{\mu_{n+1} - \mu_n} \to \delta = 4.669 \tag{4}$$

and hence, the domains of stability vanish geometrically ($\mu_{n+1} - \mu_n \propto \delta^{-n}$) and the sequence of bifurcations stops at a finite value $\mu=\mu_c$ such that for $\mu > \mu_c$ one has chaotic behavior. The theoretical and experimental domains over which the periodic waveforms in Fig. 2 are observed are given in Fig. 4. The experimental bifurcation points are in fair agreement with theory, given the difficulty (due to critical fluctuations) of defining these points experimentally (the different chaotic domains also show qualitative agreement with numerical estimates of the domains). The ratio of the period-two domain to period four is 4.3 ± 0.3, which is in qualitative agreement with Feigenbaum's hypothesis, given that the scaling is only approximate for low periods.

In terms of the gross features of the bifurcations, the experiment is in good agreement with the period-doubling and universality ideas, except for the absence of period doublings from period eight on. While we observe period two and period four

with complete reliability, we observe period eight only rarely (i.e., less than 1% of the times that we sweep through the bifurcation sequence), and we never observe periods sixteen and higher. It is not a straightforward matter to determine whether these observations are in conflict with the period-doubling hypothesis. First, by Eq. (4), the domains of higher period shrink rapidly. Moreover, as we discuss in Appendix A, the domain of highly stable period-eight behavior shrinks even more rapidly than Eq. (4) predicts. A crucial question, then, is whether our device is stable enough to stay in this small domain, given the fact that our laser power drifts sometimes by several percent, due to thermal effects. We contend that this cannot be the basic reason why we observe period eight so rarely, since the experimentally observed domain of frequency locking is smaller than the period-eight domain predicted by Eq. (4) ($\mu_3-\mu_2=0.016$). While frequency-locked behavior is occasionally erratic, it is usually quite well behaved, and we can see a stable substructure over still smaller domains.

An explanation of the results may lie in the fact that our optical bistable device obeys Eq. (1), i.e., a nonlinear difference-differential equation, rather than Eq. (2). No systematic mathematical studies of such equations have been reported in the literature to our knowledge. Limited numerical calculations of Eq. (1) have been given in Ref. (3) and we have been shown a number of other numerical results.[15,16] We have also been informed of an analytic study of these equations currently in progress.[16] These are preliminary results only and we were informed of them after our experiment was finished. Moreover, these results do not agree with each other on the issue of period eight. Chow[16] contends that the nonobservation of higher periods is inherent in the bifurcation structure of Eq. (1) due to its differential nature and we are observing precisely what the equation predicts. Ikeda's numerical results[15] show a period-eight behavior. Chow also asserts that the following can be demonstrated analytically:

(1) The sequence of period doubling terminates after a finite number of bifurcations at a point $\mu=\mu^*<\mu_c$. The termination point is not universal and occurs in our case near the point $\mu=\mu_2$ (the latter is a numerical result), i.e., at the bifurcation between period four and period eight.

(2) For $\mu^*\leq\mu\leq\mu_c$, the chaotic output is what we call period-four chaos.

(3) For special initial conditions and special μ, the higher periods can be seen, but this is a very improbable occurrence.

(4) The mixed-amplitude state (see Appendix A) is unstable, and it decays into the square wave.

(5) There should be strong "overshoots" appearing on the periodic waveforms prior to going over to chaos.

These results apply independently of τ (provided $\tau<<t_R$) and they do not go over into a case described by Eq. (2) in the limit $\tau\rightarrow 0$.

Our experimental results are in complete agreement with these predictions. With respect to item (3), we observe period eight perhaps once in every few hundred to one thousand attempts (we have seen it three times) in a fashion independent of the device stability and the level of noise. In this regard, it has been demonstrated in a hydrodynamic experiment that the observed bifurcation structure is very insensitive to noise.[20]

On the other hand, the noise levels of the experiment and the slow convergence times of our device in the domain of interest also permit an explanation in terms of critical fluctuations. This explanation and why we feel it should be considered as a possibility are given in Appendix A.

Let us turn next to the chaotic domain and restrict our discussion to the case $\mu<1$, since for $\mu>1$ the trajectories are no longer confined to separate domains centered about the upper and lower branches of Fig. 4. A chaotic trajectory of Eq. (2) starting from initial point $X=X(0)$ is defined as having the property that a neighboring trajectory starting from $X=X(0)+\delta X$ diverges exponentially from it.[12] Within the chaotic domain, Eq. (2) has both chaotic and periodic solutions, where the periodic solutions have odd periods. We have observed these odd-period solutions only when the device was not properly aligned. From private communication,[15] we are led to believe that odd-period solutions of Eq. (1) do not actually occur in the chaotic domain. Furthermore, our calculations show that these periodic solutions of Eq. (2) should not exist in the presence of the level of noise in our experiment (which comes from the digitization accuracy of A to D and D to A steps).

We therefore assume that we can ignore the periodic solutions of Eq. (2) for $\mu>\mu_c$, in which case the theory[18] of the chaotic domain of Eq. (2) is straightforward. As μ is increased, one finds that the domain of X over which the chaotic solution wanders is subdivided into 2^n sub-domains

which we have called "period-2^n" chaos. The way the chaotic solution changes with increasing μ reverses the order of period doubling, i.e., n decreases with increasing μ. The ordering in magnitude of the 2^n consecutive amplitudes (starting with the smallest) is the same as the ordering in the periodic solution of 2^n. Hence period-four chaos is expected to have the sequencing of Eq. (3), and should look like a period-four solution with a superimposed chaotic background. This is just what is observed. The value of μ at which period-two chaos becomes period-one or fully-developed chaos has received considerable attention in the mathematical literature,[19] since it is the point at which transients of odd period become possible. We observe the frequency-locked behavior at this boundary, which sometimes has subharmonic components of period three (these are usually not stable for long times). Since this case has periods related to τ rather than to t_R, the waveforms should not be related to any mathematical properties of Eq. (2). Ikeda's preliminary results[15] show the existence of frequency-locked behavior at this point (he sees it at $\mu=0.8$ which agrees with experiment to within the experimental error), but his theoretical frequency spectra are quite different from our experimental results.

We have compared the experimental histograms shown in Fig. 2 directly with histograms generated by Eq. (2). We find that there is some agreement on the basic structure, but many details are different. The domains of zero amplitude in period-four and period-two chaos agree quite well. The singularities at $X=0$ and $X=X_{\max}$ are expected theoretically in all chaotic cases of $\mu<1$, and are seen experimentally only in the cases of period-two and period-four chaos. There are additional theoretical peaks which are not systematically observed. The histogram of fully developed chaos (row six in Fig. 2) is in poor agreement with theory, which predicts a histogram that looks very much like the histogram of frequency-locked behavior shown in row five.

The relationship between the chaotic solutions of Eq. (2) and the resulting solutions of Eq. (1) have been discussed in Ref. 3. Because nearby chaotic trajectories diverge exponentially, and because initial amplitudes of $X(t)$ are never precisely constant in time, chaos implies that the amplitude cannot remain constant over a time t_R. Instead, it must break up into short-time-scale behavior that is stabilized by the time scale τ. This is quite different from the effect of small-amplitude noise on the periodic solutions. There the fluctuations are large only when the response time of the device is very slow due to critical slowing down (See Appendix A). Hence, noisy fluctuations occur on time scales t_R or larger. For $\tau<<t_R$, these are easily distinguished from each other. The only ambiguity is discussed in Appendix A, in which "mixed-amplitude" transients, rather than noisy transients, cause the confusion.

IV. CONCLUSION

In summary, we have observed, in detail, the bifurcation structure in an optically bistable hybrid. In a general sense, this structure is in good agreement with theory. The system bifurcates to chaos through two period doublings. The ratios of the domains of the doublings and of the Fourier amplitudes of the spectra are in adequate quantitative agreement with Feigenbaum's[14] universal coefficients δ and α (see Appendix A) given that the scaling relations that lead to these coefficients are only approximate for low periods. We rarely observe the predicted bifurcation to period eight, and we never observe bifurcations to period sixteen or higher. A recent calculation suggests[16] that this is a generic property of Eq. (1) and is not a defect in the experiment. From an experimental point of view, our difficulties with the higher periods are also equally compatible with the notion that critical fluctuations obscure the phenomenon, rather than there being any intrinsic defect in using Feigenbaum's analysis in this case. The observation of these fine details of the bifurcation structure will be greatly aided by using a very fast hybrid that will allow for an all-electrical or optical delay line. The computer is the chief source of fluctuations (digitization noise) and the *A-D*, *D-A* steps cannot be made fast enough so that we can look at the spectrum in real time. This measurement would greatly clarify whether or not higher-period bifurcations occur.

The overall structure of the chaotic domain follows the reverse-bifurcation scheme discussed by Lorenz.[17] One see partially developed chaos first, with an overlying period-four and period-two waveform, and only for larger input intensities is fully developed chaos observed. The statistical properties of the chaos are in reasonable agreement with theory except for the histogram of fully developed chaos.

Between the partially and fully developed chaotic domains, we see a new frequency appear that is

clearly associated with the response time (bandwidth) of the feedback loop. Hence, this is a special property of the difference-differential equation and it has been recently found theoretically.[15] The new frequency is observed to lock to a high harmonic of the period-two frequency. Such frequency-locked behavior is commonly observed in hydrodynamic turbulence,[7] and it is interesting that it occurs in a system as simple as ours.

One of the urgent matters in the near future is an experiment that determines whether the Ikeda instability occurs in an optical cavity. Our experiment is encouraging in that regard, since the example we consider here has the property that the time-average behavior of our device is very different from what is predicted if the instability is absent. This suggests looking for the instability using pulsed lasers with rapidly relaxing nonlinearities and very short cavities for which it may be difficult to resolve the instability in time. In addition, we find that instability exists, with a substantial modification in domains, even for relaxation times that are more than two times longer than the delay time. This is encouraging news from the standpoint of doing a cavity experiment using cw lasers and media with relaxation times in the nanosecond range, and also for the possibility of building practical all-optical oscillators.

Note added in proof. Dr. Ikeda has brought to our attention the article by J. Crutchfield, M. Nauenberg, and J. Rudnick, Phys. Rev. Lett. 46, 933 (1981), which shows that the bifurcation sequence can be truncated by noise in a manner that is consistent with our experimental results. Our recent experiments with a fast hybrid have suggested that this is an important, and perhaps the dominant mechanism for eliminating period eight.

ACKNOWLEDGMENTS

We would like to give special thanks to K. Ikeda and S. N. Chow for communicating the results of their calculations. We thank P. Fife, J. P. Gollub, and J. Guckenheimer for useful discussions. This work was supported by the National Science Foundation under Grant No. PHY 8104982.

APPENDIX A

An alternative explanation for the fact that we can observe period eight only rarely may lie in the existence of critical fluctuations in the system. Since the bifurcations are nonequilibrium phase transitions, it follows that, near the bifurcation points, the system approaches the asymptotic state very slowly, and the waveforms are observed to be noisy (i.e., there are critical fluctuations). The noisiness of the waveforms is the chief source of uncertainty in precisely locating the bifurcation points. As the system bifurcates to higher periods, one expects that the recovery time will increase in proportion to the period (this follows from the scaling). Since the noisiness is a function of the recovery time, as the system goes to higher periods an ever increasing percentage of the domain will be subject to critical fluctuations. Near the center of each domain, there is a small sub-domain in which the waveform recovers very quickly. Following Feigenbaum,[14] we call this a "superstable" waveform (this is also often referred to as a "critical orbit"[1]). In light of the previous remarks, the portion of the domain that is superstable shrinks quite rapidly with increasing μ.

By itself, this increasing sensitivity to fluctuations is not enough to rule out period eight, since it is fairly easy to distinguish noisy traces from chaotic ones. There is, however, a transient waveform that is very annoying, which occurs when several of the stable amplitudes occur within one time t_R. For example, in the case of period two, one could have the sequence $\bar{X}_1^{(2)},\bar{X}_2^{(2)},\bar{X}_1^{(2)}$ occur within a time t_R followed by $\bar{X}_2^{(2)},\bar{X}_1^{(2)},\bar{X}_2^{(2)}$ within the next t_R, etc. Equation (2) by itself allows such behavior, but the numerical calculations[3,15] and experimental evidence show that the stable waveform of Eq. (1) has $\bar{X}_1^{(2)}$ for one t_R followed by $\bar{X}_2^{(2)}$ for the next t_R, i.e., a square wave, (see also Sec. III for a report of Ref. 16). There is no theory to guide us here in determining how rapidly these mixed-amplitude transients should decay, but we have substantial experimental evidence from the period-two and period-four behavior that suggests that these are likely to decay very slowly, and hence they will be a major source of difficulty with period eight. As a rule, mixed-amplitude transients are observed to decay at a much slower rate than the rate at which the steady-state amplitudes are established. They also decay much more slowly in the period-four case than in period two. Finally, within the period-four domain, waveforms in which the nearest-neighbor amplitudes (e.g., $\bar{X}_1^{(4)},\bar{X}_3^{(4)}$) are mixed decay much more slowly than the ones on which the more distant ones (e.g., $\bar{X}_1^{(4)},\bar{X}_4^{(4)}$) are mixed. We also note that the scaling rule implies that the nearest-neighbor amplitudes that come in with peirod eight are closer together

compared to those amplitudes of period four. This is stated quantitatively by noting that the new Fourier amplitudes that appear at $\omega=(2^n t_R)^{-1}$ for the nth bifurcation fall off as α^{-n} where $\alpha=2.9$ is a universal constant related to δ.[14] The existence of long-lived mixed-amplitude transients would account for our difficulties in seeing period eight. The problem here is one of perception, namely, that a noise-driven mixed-amplitude transient (we have observed this noise-driven process directly) and period-four chaos are difficult to distinguish with our apparatus. Moreover, we are puzzled by the fact that when we do find period-eight waveforms, then they are extremely long lived; we would have anticipated that in light of their inherent improbability [item (3) in Sec. III] and their observed noisiness, that they simply should not exist at all if the theory of Ref. 16 is right. We are currently constructing a much faster version of our device and this will enable us to examine the spectrum in real time which should resolve these questions.

---

[1]For numerous discussions of chaos in many different disciplines, see, *Bifurcation Theory and Applications in Scientific Disciplines*, edited by O. Gurel and O. E. Rossler (New York Academy of Sciences, New York, 1979). See also R. May, Nature (London) 261, 459 (1976), and references cited therein.

[2]K. Ikeda, Opt. Commun. 30, 257 (1979).

[3]K. Ikeda, H. Daido, and O. Akimoto, Phys. Rev. Lett. 45, 709 (1980).

[4]H. Seidel, U. S. Patent No. 3 610 731 (5 October 1971). A. Szöke, V. Daneu, J. Goldhar, and N. A. Kurnit, Appl. Phys. Lett. 15, 376 (1969); S. L. McCall, Phys. Rev. A 9, 1515 (1974); M. Spencer and W. E. Lamb, Jr., Phys. Rev. A 5, 864 (1972); H. M. Gibbs, S. L. McCall, and T. N. C. Venkatesan, Phys. Rev. Lett. 19, 1135 (1976). H. M. Gibbs, T. N. C. Venkatesan, S. L. McCall, A. Passner, A. C. Gossard, and W. Wiegmann, Appl. Phys. Lett. 35, 451 (1979); D. A. B. Miller, S. D. Smith, and A. Johnston, *ibid.* 35, 658 (1979). *Optical Bistability*, edited by C. M. Bowden, M. Ciftan, and H. R. Robl (Plenum, New York, 1981).

[5]H. M. Gibbs, F. A. Hopf, D. L. Kaplan, and R. L. Shoemaker, Phys. Rev. Lett. 46, 474 (1981).

[6]P. R. Fenstermacher, H. L. Swinney and J. P. Gollub, J. Fluid Mech. 94, 103 (1979).

[7]J. P. Gollub and S. V. Benson, J. Fluid Mech. 100, 449 (1980).

[8]J. Maurer and A. Lebehabe, J. Phys. Lett. (Paris) 40, 419 (1979).

[9]B. A. Huberman, J. P. Crutchfield, and N. H. Packart, Appl. Phys. Lett. 37, 750, 1980; F. C. Moon and P. J. Holmes, J. Sound Vib. 65, 275 (1979).

[10]An examination of the bifurcation structure of coupled oscillator circuits is given by J. P. Gollub, E. J. Romer, and J. E. Socolar, J. Stat. Phys. 23, 321 (1980).

[11]L. Landau, C. R. Acad. Sci. URSS 44, 311 (1944); L. Landau and E. M. Lifshitz, *Fluid Mechanics* (Academic, Reading, Mass., 1959), pp. 103–107.

[12]D. Ruelle and F. Takens, Commun. Math. Phys. 20, 167 (1971).

[13]C. Julia, J. Math. Pure Appl. 4, 47 (1918).

[14]M. J. Feigenbaum, Los Alamos Science 1, 4 (1980).

[15]K. Ikeda (private communication).

[16]S. N. Chow (unpublished).

[17]E. N. Lorenz, in *Nonlinear Dynamics*, edited by R. H. G. Hillmann (New York Academy of Sciences, New York, 1980). Note that this theory is worked out for the case of the parabolic map and it is unclear how to generalize it to our case.

[18]M. Gronchi, V. Benza, L. A. Lugiato, P. Meystre, and M. Sargent III, Phys. Rev. A 24, 1419 (1981).

[19]Ty Li and J. A. Yorke, Am. Math. Monthly 82, 985 (1975).

[20]J. P. Gollub and J. F. Steinman, Phys. Rev. Lett. 45, 551 (1980).

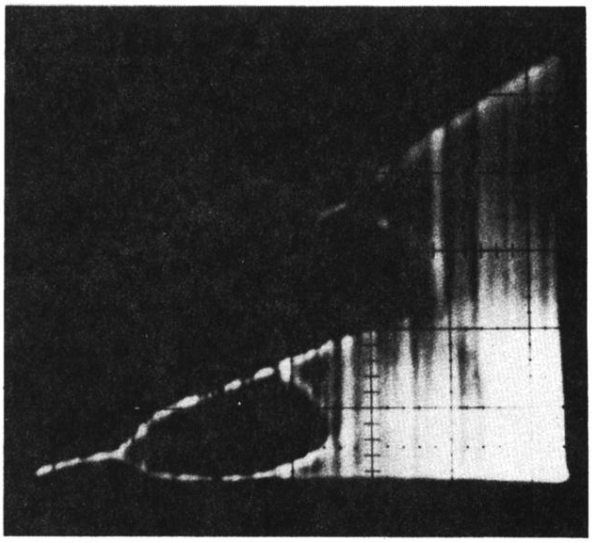

(a)

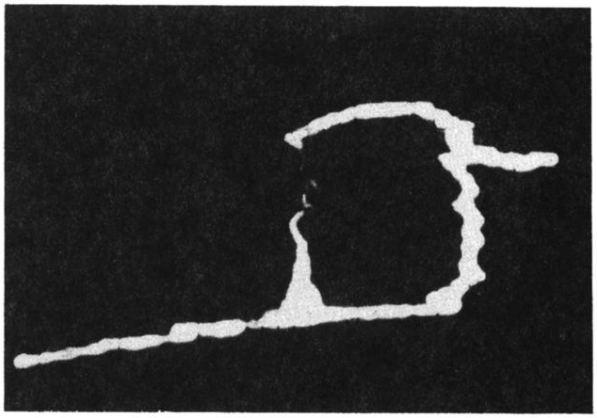

(b)

FIG. 3. (a) Output voltage V, which is mostly time dependent and hence multivalued vs input laser intensity, where the input intensity is cycled from zero to a maximum ($\mu > 0$) and back to zero. (b) Same as (a) except the vertical axis is the time average voltage on the same scale as (a).